C58

The type II inositol 1,4,5-trisphosphate receptor couples to hTrp1 rapidly enough to account for the activation of store-mediated calcium entry in human platelets

Sharon L. Brownlow and Stewart O. Sage

Department of Physiology, University of Cambridge, Cambridge CB2 3EG, UK

In human platelets, depletion of the intracellular Ca^{2+} stores by treatment with thapsigargin (TG) or thrombin results in the *de novo* coupling of the type II inositol 1,4,5-trisphosphate receptor (IP_3RII) to the putative store-operated Ca^{2+} channel, hTrp1 (Rosado & Sage, 2000*a*). This has led us to suggest that store-mediated Ca^{2+} entry (SMCE) in platelets may be activated by this coupling event. An essential requirement of this hypothesis is that protein coupling occurs rapidly enough to account for the observed Ca^{2+} entry. Here we have examined the latencies of divalent cation entry and the coupling of IP_3RII to hTrp1 in human platelets stimulated with thrombin.

Blood was drawn from healthy, drug free volunteers with local ethical committee approval and fura-2-loaded platelets prepared as previously described (Rosado & Sage, 2000*a*). The latency of thrombin-evoked Mn^{2+} entry was determined using a single mix stopped flow system with an excitation wavelength of 360 nm and emission at 500 nm. Mixing cells with agonist-free buffer was without effect on fura-2 fluorescence. To investigate coupling of IP_3RII to hTrp1, platelets were stimulated with thrombin for varying times (at 100 ms intervals) and then quenched with a lysis buffer (Rosado & Sage, 2000*a*) using a rapid quench flow system. Lysed samples were then subjected to immunoprecipitation using either an anti-hTrp1 or anti-IP_3RII antibody and co-immunoprecipitation probed for by Western blotting with the reciprocal antibody following SDS–PAGE (Rosado & Sage, 2000*a*). Coupling was absent in resting platelet preparations, and samples mixed with agonist-free buffer. All experiments were conducted at 37 °C.

Thrombin at final concentrations of 0.1 or 1 unit ml^{-1} evoked Mn^{2+} entry (in the presence of 100 μM Mn^{2+} and 1 mM EGTA) with a delay of 1.36 ± 0.09 or 0.81 ± 0.07 s, respectively (means ± S.E.M., $n = 7$). At thrombin concentrations of 0.1 or 1.0 unit ml^{-1}, co-immunoprecipitation of IP_3RII with hTrp1was first detected at 1.4 s ($n = 4$) or 0.9 s ($n = 8$), respectively. We have found that thrombin at high concentrations (10 units ml^{-1}) can evoke Ca^{2+} entry independently of Ca^{2+} store depletion, but dependent on the activation of protein kinase C (PKC; Rosado & Sage, 2000*b*). To exclude the possibility that this PKC-dependent pathway contributed to the divalent cation entry evoked by 1 unit ml^{-1} thrombin, the experiments were repeated using cells with or without a 5 min pre-treatment with the PKC inhibitor Ro-31-8220 (5 μM, a concentration sufficient to block divalent cation entry evoked by 1 μM phorbol myristate acetate). The delay in the onset of Mn^{2+} entry (in the presence of 1 mM extracellular Ca^{2+}) evoked by 1 unit ml^{-1} thrombin was 0.83 ± 0.02 s in the absence of Ro-31-8220 and 0.85 ± 0.00 s in its presence ($n = 10$). This difference was not significant (Student's paired *t* test, $P = 0.39$). Coupling of IP_3RII to hTrp1 was first detected at 0.9 s in the presence or absence of Ro-31-8220.

These results indicate that thrombin evokes the coupling of IP_3RII to hTrp1 rapidly enough for this to mediate the activation of SMCE in human platelets.

Rosado JA & Sage SO (2000*a*). *Biochem J* **356**, 191–198.

Rosado JA & Sage SO (2000*b*). *J Physiol* **529**, 159–169.

This work was supported by the Wellcome Trust (064070).

All procedures accord with current local guidelines and the Declaration of Helsinki.

C59

Sarcolemmal acid extruders affect Ca_i^{2+} signalling during acidosis in mammalian ventricular myocytes

Emma Dilworth, Tyara Banerjee and Richard D. Vaughan-Jones

Burdon Sanderson Cardiac Science Centre, University Laboratory of Physiology, Parks Road, Oxford OX1 3PT, UK

Intracellular acidosis can increase evoked Ca_i^{2+}-transient amplitude (e.g. Choi *et al.* 2000). We have examined the role played by sarcolemmal Na^+–H^+ exchange (NHE) and Na^+–HCO_3^- cotransport (NBC).

Ventricular myocytes, isolated from guinea-pig and rat (humanely killed by cervical dislocation), were AM-loaded with Fluo-3, and field stimulated at 0.3 Hz. Acetate (80 mM) was superfused to reduce pH_i. In parallel experiments, pH_i was monitored (AM-loaded carboxy SNARF-1). All experiments were conducted at 37 °C. Results are expressed as means ± S.E.M. and *P* values were calculated with Student's paired *t* test.

With Hepes-buffered superfusates, reducing pH_i by 0.46 ± 0.02 pH units ($n = 17$) activated NHE. In guinea-pig myocytes, there was an initial 20 % decrease in Fluo-3 fluorescence-transient amplitude and then, within 90 s, a secondary increase to 121 ± 9.4 % ($n = 9$) of control, despite continuing acidosis. In the presence of the selective NHE-1 inhibitor, cariporide (30 μM), the secondary increase (now from 77% to 80 ± 3.7 % of control; $n = 9$) was significantly inhibited ($P < 0.05$). Similar results were obtained with rat myocytes ($n = 10$, $P < 0.05$). Thus, NHE activity is involved in the acid-induced increase in Ca_i^{2+}-transient amplitude.

With 22 mM HCO_3^-–5 % CO_2-buffered superfusates, reducing pH_i by 0.28 ± 0.01 pH units ($n = 25$) activated both NHE and NBC. In guinea-pig myocytes, there was an initial 15 % decrease followed by a secondary increase that was maximal 2–3 min after adding acetate (amplitude 116 ± 0.03 % of control, $n = 9$), despite the continuing acidosis. In 30 μM cariporide, after the initial decrease, the transient amplitude displayed some recovery (to 94 ± 0.04% of control, $n = 8$), but significantly less than in acetate alone ($P < 0.05$). In the presence of both cariporide and 10 μM S0859, a selective NBC inhibitor (Chen & Vaughan-Jones, 2001) there was a further significant reduction in amplitude at 2–3 min (now to 79 ± 0.03% of control, $n = 11$, $P < 0.05$), such that there was virtually no recovery from the initial decrease. In the rat, cariporide similarly attenuated the secondary recovery ($n = 6$, $P < 0.05$), but there appeared to be no additional inhibitory effect of adding S0859 ($n = 7$). Therefore during acidosis in the guinea-pig but not the rat, NBC activity is also involved in the acid-induced rise of systolic Ca_i^{2+}.

The increase of systolic Ca_i^{2+} during acidosis is not due to recovery of pH_i, which remained acidic over the time period. It is most likely driven by a rise of Na_i^+ through Na^+ influx on NHE and NBC. By acting on sarcolemmal Na^+–Ca^{2+} exchange, this can indirectly increase SR Ca^{2+} loading and release. The greater part of the Ca_i^{2+}-transient increase appears to depend on NHE activity although, in guinea-pig myocytes, a smaller involvement of NBC is apparent. The stimulatory effect of NHE and NBC on Ca_i^{2+} will help to counteract the inhibitory effect of intracellular acidosis on contraction.

Ch'en FF & Vaughan-Jones RD (2001). *Proc 34th Int Congress of Physiological Sciences* A1495 (abstract)

Choi HS *et al* (2000). *J Physiol* **529**, 661–668.

This work was funded by the BHF and Wellcome Trust. We thank Dr H. Kleeman of Aventis, for kindly providing cariporide and S0859

All procedures accord with current UK legislation.

C60

Steady-state and dynamic relationship between intracellular pH and active shortening in isolated ventricular myocytes

Pawel Swietach and Richard D. Vaughan-Jones

Burdon Sanderson Cardiac Science Centre, University Laboratory of Physiology, Parks Road, Oxford OX1 3PT, UK

The effect of intracellular pH on active shortening was studied in ventricular myocytes isolated enzymically from guinea-pig and rat (humanely killed by cervical dislocation). pH_i was measured with carboxy-SNARF-1 (AM-loaded), and active shortening was recorded simultaneously using edge-detection (pacing at 1 Hz).

To quantify the steady-state pH_i–shortening relationship, cells were superfused with various concentrations of ammonium (7.5–30 mM) or acetate (10–80 mM) at pH 7.4 and 37 °C (guinea-pig $n = 365$, rat $n = 123$). Sarcolemmal acid/base transport was largely suppressed by superfusing with Hepes-buffered solutions containing 30 μM cariporide (inhibits Na^+–H^+ exchange, NHE). Intracellular acidosis depressed contraction. The pH_i–shortening relationship, evaluated for steady-state pH_i and contraction, was sigmoidal with a Hill coefficient of 1.91 (guinea-pig) and 1.35 (rat), centred around resting pH_i (for multicellular tissue, see Bountra & Vaughan-Jones, 1989).

To study the dynamic pH_i–shortening relationship, shortening and pH_i were measured during and after a 4 min exposure to 40 mM acetate. In order to establish the effect of sarcolemmal acid/base transport and intracellular buffering capacity, the protocol was executed in Hepes- or CO_2/HCO_3^--buffered medium, and in the presence of 10 μM S0859 (inhibits Na^+–HCO_3^- co-transport, NBC; Ch'en & Vaughan-Jones, 2001) and/or 30 μM cariporide (guinea-pig $n = 8$–52, rat $n = 7$–25). Shortening displayed a clockwise hysteresis against pH_i in the acid range (acetate addition) and in the subsequent alkaline range (acetate removal).

Acid hysteresis persisted after inhibition of NHE and NBC (guinea-pig, rat $n = 7$–18) or after imposition of CO_2/HCO_3^--buffered conditions (guinea-pig $n = 38$, rat $n = 22$). It may be caused by changes in pH_i-sensitive Ca^{2+} fluxes at the sarcoplasmic reticulum and the sarcolemma exerting opposite effects on contraction, and with lesser or greater time delays, respectively.

Alkaline-hysteresis was large in Hepes-buffered superfusates. It was collapsed in the presence of NHE and NBC inhibitors (guinea-pig, rat $n = 7$–18). It was also collapsed in the presence of CO_2/HCO_3^- buffer (guinea-pig $n = 38$, rat $n = 22$). Alkaline-hysteresis may be caused by a kinetic mismatch between changes of $[Na^+]_i$ and pH_i under these conditions, given that each of these parameters is a major modulator of contraction.

In conclusion, active shortening displays considerable pH_i sensitivity, although the dependence during dynamic changes of pH_i depends on the immediate pH_i history of the myocyte.

Bountra C & Vaughan-Jones RD (1989). *J Physiol* **418**, 163–187.

Ch'en FFT & Vaughan-Jones RD (2001). *Proc 34th Int Congress of Physiological Sciences* A1495 (abstract).

This work was funded by the BHF, Wellcome Trust and ORS. We thank Dr H.-W. Kleeman of Aventis for kindly providing cariporide and S0859.

All procedures accord with current UK legislation.

C63

Depolarisation markedly potentiates P2Y receptor-evoked Ca^{2+} responses at low agonist concentrations via a dihydropyridine-insensitive mechanism

Iman S. Gurung and Martyn P. Mahaut-Smith

Department of Physiology, University of Cambridge, Cambridge, UK

A significant body of evidence now suggests that signalling via certain G-protein-coupled receptors (GPCRs) can be directly regulated by the membrane potential. The most extensively studied example is the bipolar voltage control of P2Y receptor-evoked Ca^{2+} release in non-excitable rat megakaryocytes (MKs), a phenomenon that requires functional IP_3 receptors (Mason & Mahaut-Smith, 2001). We have now examined (i) the agonist dependence of this phenomenon and (ii) the role of dihydropyridine receptors (DHPRs).

Adult male Wistar rats were humanely killed by exposure to a rising concentration of CO_2 followed by cervical dislocation. Combined whole-cell patch clamp and fura-2 fluorescence recordings from marrow MKs were conducted as previously described (Mason & Mahaut-Smith, 2001). ADP was superfused at a near-threshold concentration of 0.01 or 0.03 μM, and also at 1 μM and 100 μM. In cells showing an agonist-evoked Ca^{2+} increase at all concentrations, depolarisation (80 mV, 10 s from −75 mV) stimulated a larger Ca^{2+} increase in 0.01/0.03 μM ADP (340 ± 58 nM, mean ± S.E.M., $n = 13$) than in 1 μM ADP (139 ± 16 nM, $n = 23$) or in 100 μM ADP (75 ± 26, $n = 7$). Interestingly 6/10 cells that failed to respond to 0.01/0.03 μM ADP alone, showed a large Ca^{2+} increase following depolarisation (239 ± 35 nM).

In megakaryocytes exposed to 1 μM ADP, the Ca^{2+} increase evoked by depolarisation (80 mV, 10 s from −75 mV) was not significantly different ($P > 0.05$, Student's unpaired t test) in the presence of 50 μM nifedipine (196 ± 23 nM, $n = 19$) compared to controls (161 ± 30, $n = 19$). Nifedipine caused a substantial block of the voltage-dependent outward K^+ current and thereby acted as a positive control. This result contrasts with the reported complete block of the slow (IP_3-dependent) phase of the depolarisation-induced Ca^{2+} increase in skeletal muscle by 10 μM nifedipine (Araya *et al.* 2003).

Our data demonstrate that a large depolarisation-evoked Ca^{2+} release is observed during near-threshold stimulation of P2Y receptors in the megakaryocyte. In addition, in contrast to skeletal muscle, the underlying mechanism does not require DHPRs. The physiological relevance of the voltage control of P2Y receptors is unknown, but could represent a means whereby ionotropic receptors or action potentials (Martinez-Pinna *et al.* 2003) potentiate cellular activation via this and other GPCRs.

Araya R *et al.* (2003). *J Gen Physiol* **121**, 3–16.

Martinez-Pinna J *et al.* (2003). *J Physiol* **548.P**, S31.

Mason MJ & Mahaut-Smith MP (2001). *J Physiol* **533**, 175–183.

This work was funded by the BHF and MRC. I.S.G. is supported by a Gates Cambridge Scholarship and an ORS Award.

All procedures accord with current UK legislation.

C65

Anti-neoplastic action of extracellular nucleotides in transitional cell carcinoma is mediated by P2-purinergic receptors

M. Shabbir*‡, C.S. Thompson† D.P. Mikhailidis†, R.J. Morgan* and G. Burnstock‡

**Depatment of Urology, †Department of Clinical Biochemisrty and ‡The Autonomic Neuroscience Institute, Royal Free & University College Medical School, London, UK*

Bladder cancer is the second most common malignancy affecting the genitourinary tract. High-grade bladder cancer has an increased rate of tumour invasion, recurrence and progression. Despite recent therapeutic advances, it has a poor prognosis with a reduced 10-year survival (98% grade 1 *vs.* 35% grade 3). Extracellular nucleotides, such as ATP, have been shown to inhibit the growth of various adenocarcinomas including prostate cancer (Janssens & Boeynaems 2001). We undertook experiments to assess whether this anti-neoplastic activity extended to other urological malignancies by assessing the effect of purinergic agonists on the grade 3 human bladder cancer cell line HT-1376, a transitional cell carcinoma.

HT-1376 cells were grown in MEM supplemented with 8% fetal bovine serum, 1% non-essential amino acids and 1% antibiotic solution containing penicillin and streptomycin in humidified 5% CO_2 at 37°C. Culture wells were seeded at 90 000 cells per well. After 24 h (day 0) cells were treated daily with ATP (10^{-6} M to 10^{-2} M, $n = 9$ for each concentration) or without ATP (control, $n = 9$) and incubated for a further 72 h, at which stage the number of adherent viable cells that excluded trypan blue were counted using a haemocytometer. Experiments were repeated in the presence of the P1-receptor antagonist 8-sulphophenyl theophylline (ATP 10^{-4} M, 8-SPT 10^{-5} M to 10^{-4} M, $n = 6$ for each combination). The effects of the different purinergic agonists UTP, UDP, BzATP, ATPγS, 2-meSATP, 2-meSADP and α,β-meATP (all at 10^{-4} M, $n = 12$ per agonist) on cell growth were also assessed. Results are expressed as means ± S.E.M. and statistical differences are determined using Student's two-tail paired *t* test.

After 72 h the number of cells in the control group had increased 3-fold (baseline control 100 000 ± 2500 cells *vs.* 72 h control 296 000 ± 5 340 cells; $P < 0.0001$). ATP (10^{-4} M) added daily not only inhibited this proliferation, but further reduced the cell number to 19% below the baseline (72 h ATP treated wells 81 000 ± 2700 cells *vs.* 72 h control; $P < 0.0001$). This anti-neoplastic action was dose-dependent ($EC_{50} = 8.4 \times 10^{-5}$ M) and was not affected by 8-SPT indicating that ATP was acting via a P2-purinergic receptor. The rank order of agonist potency was ATPγS > ATP ⩾ BzATP > 2-meSATP. The P2X agonist α,β-meATP ($P2X_1$, $P2X_3$), and the P2Y agonists 2-meSADP ($P2Y_1$), UTP ($P2Y_2$, $P2Y_4$) and UDP ($P2Y_6$) had no anti-neoplastic effect.

Our results show, for the first time, that extracellular nucleotides completely inhibit the growth of urinary transitional cell carcinomas. This anti-neoplastic action is mediated by P2-purinergic receptors. The agonist profile and the rank order of agonist potency suggest this action is likely to be mediated by $P2X_4$, $P2X_5$, and/or $P2Y_{11}$ receptors. Exploitation of these findings may provide a potential therapeutic target for the treatment of high-grade bladder cancer.

Janssens R & Boeynaems J-M (2001). *Br J Pharm* **132**, 536–546.

M.S. is supported by a Royal College of Surgeons of England Research Fellowship Grant.

C66

On the role of D-lactate as a competitive inhibitor for astrocyte to axon transfer of L-lactate in a central white matter pathway

Selva Baltan Tekkök*, Angus M. Brown*† and Bruce R. Ransom*

**Department of Neurology, University of Washington, Seattle, WA 98195, USA and †MRC Applied Neuroscience Group, Biomedical Sciences, University of Nottingham, Nottingham NG7 2UH, UK*

Metabolic coupling between glial cells and neurones was first recognised in the honey bee retina, where glial cells released alanine, which is taken up and oxidatively metabolised by photoreceptors (Tsacopoulos *et al.* 1994). Analogous studies have since demonstrated similar coupling in a variety of central mammalian preparations where glucose is taken up by astrocytes and metabolised to lactate, which is then shuttled to neural elements across the narrow extracellular space. In this study we used electrophysiological and pharmacological procedures to investigate the ability of D-lactate to act as a metabolically inert competitive inhibitor of astrocyte–axon intercellular L-lactate transport in the adult mouse optic nerve (MON), a typical central white matter tract.

Adult male Swiss Webster mice (20–25 g) were killed by decapitation under deep anaesthesia with CO_2. The optic nerves were placed in an interface perfusion chamber with oxygenated aCSF at 37°C. All experiments were carried out in accordance with the guidelines for Animal Care of the University of Washington. Data are presented as means ± S.E.M. and Student's unpaired *t* test was employed to determine significance.

A 50 μs, supramaximal stimulus evoked a compound action potential (CAP) that characteristically displayed three peaks (Brown *et al.* 2003). MONs superfused with control aCSF containing 10 mM glucose had stable robust CAPs for several hours. Replacement of glucose with 20 mM L-lactate sustained the CAP for 2 h indicating that L-lactate can substitute for glucose as a metabolic substrate. During a 60 min period of aglycaemia the CAP was maintained for 22.8 ± 2.2 min ($n = 8$) before failing. The CAP could be partially rescued by subsequent superfusion with control aCSF; CAP recovered to 38.2 ± 4.2% ($n = 8$) of control. Superfusion with 20 mM D-lactate following aglycaemia did not rescue the CAP, indicating that D-lactate is metabolically inert. Aglycaemia in the presence of 20 mM D-lactate resulted in accelerated CAP decline compared to aglycaemia alone (14.4 ± 0.6 min; $n = 4$; $P < 0.05$). The CAP could be maintained in the relatively hypoglycaemic glucose concentration of 2 mM for up to 2 h, but prior depletion of glycogen rendered 2 mM glucose incapable of supporting function, suggesting that astrocytic glycogen was supplementing glucose to support function. Addition of 150 μM cinnemate or 20 mM D-lactate in the presence of 2 mM glucose resulted in loss of the CAP after 7.9 ± 2.2 min ($n = 3$) or 18.3 ± 0.4 min ($n = 3$), respectively.

These results indicate that in the MON L-lactate is transferred between astrocytes and axons. Glycogen-derived L-lactate presumably sustains axon function either in the absence of glucose, or when ambient glucose is insufficient to meet axonal energy requirements. D-Lactate is a valuable new pharmacological tool to probe the metabolic coupling between astrocytes and neural elements as it has no apparent secondary effects (cf. cinnemate) and is metabolically inert.

Brown AM *et al.* (2003). *J Physiol* **549**, 501–512.

Tsacopoulos M *et al.* (1994). *J Neurosci* **14**, 1339–1351.

This work was supported by NIH Grant 15589 (BRR) and the EPVA (AMB & BRR).

All procedures accord with current local guidelines.

C67

Insulin increases the expression of cationic amino acid transporters 1 and 2, and endothelial nitric oxide synthase in human fetal endothelium

M. González*, R. Rojas*, P. Casanello*† and L. Sobrevia*

**Cellular and Molecular Physiology Laboratory (CMPL), Department of Obstetrics and Gynaecology & Medical Research Centre (CIM), School of Medicine, Pontificia Universidad Católica de Chile, PO Box 114-D, Santiago and † Department of Obstetrics and Gynaecology, Faculty of Medicine, University of Concepción, PO Box 160-C, Concepción, Chile*

Insulin stimulates nitric oxide (NO) synthesis, via the endothelial NO synthase (eNOS), and L-arginine transport, via the cationic amino acid transporters 1 (hCAT-1) and 2B (hCAT-2B) in human umbilical vein endothelial cells (HUVECs) (Sobrevia *et al.* 1996; Flores *et al.* 2001). Biological actions of insulin involve activation of phosphatidylinositol 3-kinase (PI3K), protein kinase C (PKC) and the mitogen-activated protein kinase (MAPK) pathway in mammalian cells (Bevan, 2001). We investigated the involvement of PI3K, PKC and p42/p44^{mapk} in the effect of insulin on activity and expression of CATs in HUVECs.

Cells were isolated (0.2 mg ml^{-1} collagenase) from normal pregnancies (Ethics Committee approval and informed patient consent were obtained) and cultured in medium 199 (M199) supplemented with sera. L-[^{3}H]Arginine transport (100 μM, 2 μCi ml^{-1}, 37 °C, 1 min) and mRNA for hCAT-1 and hCAT-2B were quantified by real time PCR in the presence or absence of insulin (0.1 nM, 8 h), wortmannin (50 nM, 30 min, PI3K inhibitor), PD-98059 (10 μM, 30 min, MAPK kinase inhibitor), calphostin C (100 nM, 30 min, PKC inhibitor) or N^G-nitro-L-arginine methyl ester (L-NAME, 100 μM, 30 min, eNOS inhibitor). The effect of insulin on p42/44^{mapk} activation was also assayed by Western blot.

Insulin increased the V_{max} (21 ± 1 *vs.* 4 ± 0.2 pmol (μg protein)$^{-1}$ min^{-1}, $n = 5$, $P < 0.05$, means ± S.E.M., Student's unpaired t test) with no significant changes in the apparent K_m (control: 138 ± 21 μM, insulin: 101 ± 21 μM, $P > 0.05$). Insulin-increased V_{max} was blocked ($P < 0.05$) by wortmannin (2.8 ± 0.6 pmol (μg protein)$^{-1}$ min^{-1}), calphostin C (2.3 ± 0.4 pmol (μg protein)$^{-1}$ min^{-1} and L-NAME (3.5 ± 0.5 pmol (μg protein)$^{-1}$ min^{-1}). Insulin also increased hCAT-1 (3-fold) and hCAT-2B (1.7-fold) mRNA number of copies, effects that were blocked ($P < 0.05$) by PD-98059 and calphostin C. Insulin also increased eNOS mRNA number of copies (2.3-fold) and protein (1.7-fold) level, and eNOS activity (2.1-fold), and induced phosphorylation of p42/44^{mapk}.

In summary, increased activity of L-arginine transport induced by insulin involves PI3K, PKC and eNOS activity in HUVECs. In addition, insulin-induced increase of L-arginine transport may be due to increased expression of hCAT-1 transporters.

Bevan P (2001). *J Cell Science* **114**, 1429–1430.

Flores C *et al.* (2001). *J Physiol* **536.P**, 167*P*.

Sobrevia L *et al.* (1996). *J Physiol* **490**, 775–781.

This work was supported by FONDECYT (1030781, 1030607, 7030004, 7030109) and DIUC-University of Concepción (201.084.003-1.0)-Chile, and The Welcome Trust (UK).

All procedures accord with current National guidelines and the Declaration of Helsinki.

C69

Evidence that accumulation of reactive oxygen species and activation of p38 mediates lipopolysaccharide-induced cell death in rat hippocampus

Y. Nolan, E. Vereker and M.A. Lynch

Department of Physiology, Trinity College, Dublin 2, Ireland

Lipopolysaccharide (LPS), a component of the cell wall of Gram-negative bacteria, has been shown to lead to neurodegenerative changes in the hippocampus. This study aims to investigate the signalling events induced by LPS which contribute to these changes.

Male Wistar rats were anaesthetized by intraperitoneal injection of urethane (1.5 g kg^{-1}), injected with SB203580 (50 μM; 5 μl) or saline (5 μl) intracerebroventricularly and 5 min later injected intraperitoneally with LPS (200 μg kg^{-1}) or saline. Three hours later rats were killed humanely by decapitation, hippocampus was dissected and frozen.

LPS increased the number of cells exhibiting fragmented DNA (assessed by TUNEL), which is indicative of degeneration, compared to saline-treated rats (Table 1; $n = 5$). This was paralleled by p38 activation where densitometric analysis of Western immunoblots confirmed a significant effect of LPS ($n = 6$). Immunocytochemical analysis of cytospun cells demonstrated an increase in the percentage of cells displaying activated p38 immunoreactivity in rats treated with LPS ($n = 5$). We also provide evidence of co-localization of activated p38 and caspase-3 in hippocampal cells after LPS treatment. Moreover, the stimulatory effect of LPS on activation of caspase-3, an indicator of cellular degradation, was abolished by pretreatment with the p38 inhibitor SB203580 ($n = 6$). LPS increased the accumulation of reactive oxygen species (ROS; $n = 6$) while incubation of tissue with H_2O_2 (200 μM), which induces the formation of ROS, increased p38 activity ($n = 6$). In addition, H_2O_2-induced activation of caspase-3 was abrogated by SB203580 ($n = 6$).

	Saline	LPS	LPS+SB
TUNEL (% +ve cells)	27.0±3.3	52.9±5.6**	
CASPASE-3 (nmol AFC/mg/min)	0.1±0.02	0.24±0.02**	0.12±0.01
p38 (arbitrary units)	8.3±0.35	9.47±0.35*	
p38 (% +ve cells)	4.0±1.9	23.9±2.7**	
ROS (nmol DCF/mg)	5.73±1.4	14.3±4.1**	
	Control	H_2O_2	H_2O_2+SB
CASPASE-3 (nmol AFC/mg/min)	0.6±0.11	1.036±0.02*	0.57±0.15
p38 (arbitrary units)	29.52±1.7	46.7±5.7*	

Table 1. Effects of LPS, H_2O_2 and SB203580 on TUNEL; accumulation of ROS; and activation of caspase-3 and p38 in the hippocampus. Data are means ± S.E.M. and were analysed, as appropriate, using Student's unpaired t test, or a one-way analysis of variance (ANOVA) followed by *post hoc* Student Newmann-Keuls; differences were deemed significant when $P < 0.05$. *$P < 0.05$; **$P < 0.01$.

These data identify an essential role for accumulation of ROS and activation of p38 in mediating the cellular degeneration that occurs in the hippocampus in response to LPS.

This work was funded by Enterprise Ireland.

All procedures accord with current National guidelines.

C70

β-Amyloid peptide couples to p53^{ser15} in cultured rat cortical neurons

Marie P. Fogarty and Veronica A. Campbell

Department of Physiology, Trinity College Institute of Neuroscience, Trinity College, Dublin, Ireland

β-Amyloid ($A\beta_{1–40}$), a component of the mature senile plaque in Alzheimer's disease, is proposed to contribute to the disease pathology by influencing neuronal signalling events. The aim of this study was to examine the role of the cell cycle regulatory protein, p53, in $A\beta_{1–40}$-mediated induction of the apoptotic pathway in cultured cortical neurons.

Cultured rat cortical neurons were prepared from humanely killed rats as previously described (Fogarty *et al.* 2003). Cells were exposed to aggregated $A\beta_{1–40}$ (2 μM, 5 min) and p53 activity was assessed by Western immunoblot using an anti-phospho-p53^{ser15} or anti-phospho-p53^{ser392} antibody. Bax expression was assessed by Western immunoblot using an anti-bax antibody. Caspase-3 activity and cleavage of the DNA repair enzyme, poly-ADP ribose polymerase (PARP), were assessed by immunocytochemistry using anti-active caspase-3 and anti-cleavage site-specific PARP antibodies, respectively. To assess the role of p53 in mediating the modulatory effects of $A\beta_{1–40}$ on caspase-3 activity and PARP cleavage, the cells were pretreated with the p53 inhibitor, pifithrin-α (100 nM) for 3 h. All results are expressed as means ± S.E.M. and $P < 0.05$ was considered significant.

$A\beta_{1–40}$ significantly increased mean phospho-p53^{ser15} expression from 0.99 ± 0.01 to 1.75 ± 0.19 arbitrary units (a.u.) at 5 min ($P < 0.01$, Student's paired t test, $n = 6$) and from 1.01 ± 0.26 to 1.49 ± 0.13 a.u. at 1 h ($P < 0.01$, Student's paired t test, $n = 6$). No change in expression of phospho-p53^{ser392} was mediated by $A\beta_{1–40}$; thus phospho-p53^{ser392} expression was 1.00 ± 0.03 a.u. in control and 0.96 ± 0.09 a.u. in Aβ-treated cells at 5 min, and 0.99 ± 0.08 a.u. in control and 0.98 ± 0.10 a.u. in Aβ-treated cells at 1 h ($n = 6$). $A\beta_{1–40}$ significantly increased mean bax expression from 1.00 ± 0.03 to 1.35 ± 0.09 a.u. at 6 h ($P < 0.05$, ANOVA, $n = 6$) and this was abolished by pifithrin-α (0.95 ± 0.04 a.u., $n = 6$). Aβ significantly increased the percentage of cells displaying anti-active caspase-3 immunoreactivity from 24 ± 2 % to 48 ± 2 % at 24 h ($P < 0.01$, ANOVA, $n = 6$ coverslips) and this increase was abolished by pifithrin-α (24 ± 1 %, $n = 6$ coverslips). Similarly, Aβ significantly increased the percentage of cells displaying cleaved PARP (85 kDa) immunoreactivity from 38 ± 3 % to 67 ± 3 % at 72 h ($P < 0.01$, ANOVA, $n = 6$ coverslips) and this increase was abolished by pifithrin-α (31 ± 3 %, $n = 6$ coverslips).

These results demonstrate that $A\beta_{1–40}$ induces phosphorylation of p53 in cultured cortical neurons, leading to increased bax expression, caspase-3 activation and PARP cleavage. This pathway is likely to be involved in $A\beta_{1–40}$-mediated neuronal cell death and may be of importance in Alzheimer's disease.

Fogarty MP *et al.* (2003). *Biochem J* **371**, 779–789.

This work was supported by the Health Research Board, Ireland.

All procedures accord with current National guidelines.

PC24

Desensitization of atrial GIRK current in isolated rat atrial myocytes: an experimental artefact?

Marie-Cécile Wellner-Kienitz, Kirsten Bender, Leif I. Bösche and Lutz Pott

Institut für Physiologie, Ruhr-Universität Bochum, D-44780 Bochum, Germany

Membrane current through atrial and neuronal G protein-gated inwardly rectifying K^+ (GIRK) channels undergoes a fast (acute) desensitization upon rapid activation via appropriate receptors such as the muscarinic M_2 receptor in atrial myocytes using a saturating concentration of ACh (20 μM; Fig. 1). Pre-stimulation of GIRK current by a low concentration of ACh or via A_1 adenosine receptors resulted in a reduction of current induced by 20 μM ACh ($I_{K(ACh)}$). This reflected a decrease of the desensitizing component. It is assumed that acute desensitization does not represent classic receptor desensitization but reflects either a property of the G protein cycle (Chuang *et al.* 1998), or the channel itself (Bender *et al.* 2001). In the present study we investigated interactions between GIRK current and other inwardly rectifying K^+ currents (I_{K1}, $I_{K(ATP)}$) in cultured adult rat atrial myocytes using whole cell voltage clamp.

WK rats were humanely killed in accordance with national legislation. The heart was removed and atrial myocytes were isolated by enzymatic perfusion. Cells were cultured and used experimentally for up to 1 week.

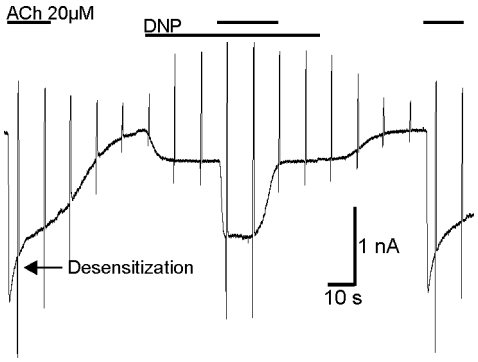

Figure 1. GIRK current elicited by rapid application of ACh (20 μM) without and with background $I_{K(ATP)}$ activated by DNP (100 μM). Rapid deflections represent changes in membrane current by voltage ramps from −120 to + 60 mV. Holding potential was −90 mV.

Activation of $I_{K(ATP)}$ by either DNP or a channel opener (chromakalim) resulted in a reduction of $I_{K(ACh)}$ and removal of its desensitizing component (Fig. 1). Overexpression of Kir2.1, one of the pore-forming subunits of I_{K1} channels, by adenoviral gene transfer caused a large constitutive inward-rectifying current paralleled by a reduction in $I_{K(ACh)}$ by $\geqslant$ 90 %. Overexpressing Kir3.4 (GIRK4) by adenoviral gene transfer, resulted in an increased constitutive (receptor-independent) GIRK current and a concomitant reduction in $I_{K(ACh)}$ and removal of its desensitizing component.

In summary, any increase in inwardly rectifying channel currents in atrial myocytes appears to result in a reduction of $I_{K(ACh)}$ amplitude and removal of the desensitizing component. As the ACh-induced hyperpolarization has similar kinetic properties as $I_{K(ACh)}$, we suggest that acute desensitization of the current is not an experimental artefact.

Bender K *et al.* (2001). *J Biol Chem* **276**, 28873–28880.

Chuang HH *et al.* (1998). *Proc Natl Acd Sci U S A* **95**, 11727–11732.

This work was supported by the Deutsche Forschungsgemeinschaft (Po212/9–3).

All procedures accord with current National guidelines.

PC25

The G protein α subunit does not determine specificity of coupling to G protein-gated inwardly rectifying K^+ (GIRK) channels

Kirsten Bender, Lutz Pott and Marie-Cécile Wellner-Kienitz

Institut für Physiologie, Ruhr-Universität Bochum, D-44780 Bochum, Germany

G protein-gated inwardly rectifying K^+ channels expressed in cardiac and neuronal cells (GIRK or Kir3.x family) are activated by interaction with $\beta\gamma$ dimers released from heterotrimeric G proteins upon stimulation of appropriate receptors. There is a controversy about whether activation in principle is limited to $\beta\gamma$-dimers released from pertussis toxin (Ptx)-sensitive G proteins. This would suggest that the α-subunit of heterotrimeric G proteins confers specificity to $G_{\beta\gamma}$ signalling, as has been proposed recently (Leaney *et al.* 2000). More recently overexpressed β_1-adrenergic receptors have been shown to couple to GIRK channels via G_s in atrial myocytes (Wellner-Kienitz *et al.* 2001).

The cardiac type of GIRK channel composed of Kir3.1/Kir3.4 was expressed by transient transfection in CHO and HEK293 cells and activation of GIRK current by different co-expressed G protein-coupled receptors was studied to address the question of whether the type of G protein confers specificity to signalling via $G_{\beta\gamma}$.

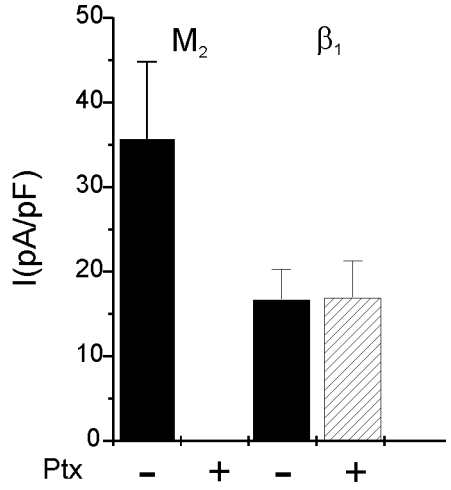

Figure 1. Normalized currents activated by either ACh (20 μM) in CHO cells expressing Kir3.1/Kir3.4 plus a muscarinic M_2 receptor or by isoprenaline (1 μM) in cells co-expressing β_1-adrenergic receptors. Comparison of control and Ptx-treated cells (2 μg ml^{-1}; 4 h). Mean values ± S.D.; $n \geqslant 10$ for each group).

Robust activation of current was observed upon stimulation of receptors coupling to $G_{i/o}$ (M_2-muscarinic, A_1-purinergic, A_3-purinergic, $S1P_2$, $S1P_3$ sphingolipid) that was completely abolished by Ptx. Via G_S coupled receptors (β_1-adrenergic, A_2 purinergic, H_2 histaminergic) currents with about 50 % less density could be activated that were insensitive to Ptx treatment (Fig. 1). Comparable results were obtained in both CHO and HEK293 cells.

These data indicate that G protein α subunits do not play a central role in determining receptor specificity of coupling to G protein-gated inwardly rectifying K^+ channels.

Leaney JL *et al.* (2000). *J Biol Chem* **275**, 921–929.
Wellner-Kienitz M-C *et al.* (2001). *J Biol Chem* **276**, 37347–37254.

This work was supported by the Deutsche Forschungsgemeinschaft (Po212/11-1).

All procedures accord with current National guidelines.

PC26

Development and modulation of cytoskeletal and synaptic proteins in acute and organotypic rat hippocampal slices

L.E. Buckby, M.R. Crompton, P.W. Beesley and R.M. Empson

School of Biological Sciences, Royal Holloway, University of London, Egham, Surrey TW20 0EX, UK

Organotypic slice cultures are being used increasingly to understand the physiology and molecular basis of synaptic plasticity (Gähwiler *et al.* 1997). Here we describe the developmental profile of cytoskeletal and synaptic marker proteins: synaptophysin (a pre-synaptic vesicle-associated protein), PSD95 (a post-synaptic protein found clustered with NMDA receptor subunits), β-tubulin (a microtubule stabilisation and growth GTPase putatively linked to NMDA receptors via PSD95) and a brain-specific neuroplastin np65 that is involved in hippocampal synaptic plasticity (Smalla *et al.* 2000).

The developmental expression of these proteins was compared in rat hippocampal acute and organotypic slices using Western blot analysis. Acute hippocampal slices were taken from humanely killed post-natal day (P)5 to adult P120 rats. Organotypic hippocampal slices, prepared from P7 rats (Stoppini *et al.* 1991), were taken between 0 and 21 days *in vitro* (DIV). Organotypic slices were cultured in control conditions or the presence of the NMDA- and/or AMPA-receptor antagonists: AP5 (100 μM) and CNQX (20 μM), respectively, for 7 DIV.

Expression of np65 in organotypic slices mimicked that in acute slices, peaking between P21–28 and 14–21 DIV. Synaptophysin and PSD95 displayed very similar developmental profiles in acute and organotypic slices rising in expression from P14 and 7 DIV onwards. β-Tubulin displayed decreasing post-natal expression in both acute and organotypic slices.

Chronic treatment of slice cultures with glutamate receptor antagonists did not affect the total expression of np65 compared with control. AP5 alone had no effect upon PSD95, synaptophysin and β-tubulin levels, although CNQX alone decreased PSD95 expression by *ca* 60 % compared with control. A synergistic effect of CNQX and AP5 together further reduced PSD95 levels to *ca* 90 % and also decreased the expression of synaptophysin and β-tubulin, both *ca* 40 % compared with control.

Our results indicate that organotypic slice cultures can be used as a reliable model to investigate functional and molecular changes in synaptogenesis and synapse stability. Furthermore chronic treatment with AMPA- and NMDA-receptor antagonists reduced the expression of PSD95, synaptophysin and β-tubulin suggesting a perturbation of synaptic function.

Gähwiler BH *et al.* (1997). *Trends Neurosci* **20**, 471–477.
Smalla K-H *et al.* (2000). *Proc Natl Acad Sci U S A* **97**, 4327–4332.
Stoppini L *et al.* (1991). *J Neurosci Methods* **37**, 173–182.

We acknowledge the support of the BBSRC (111/NEU15396).

All procedures accord with current UK legislation.

PC27

Effect of temperature and pH_i on spontaneous Ca_i^{2+} wave frequency and propagation in rat ventricular myocytes

E. Dilworth, C. Balnave and R.D. Vaughan-Jones

Burdon-Sanderson Cardiac Science Centre, University Laboratory of Physiology, Parks Road, Oxford OX1 3PT, UK

Intracellular acidosis decreases the occurrence of spontaneous Ca_i^{2+} sparks in rat ventricular myocytes (Balnave & Vaughan-Jones, 2000). Under conditions of Ca_i^{2+} overload, spark amplitude can increase, triggering arrhythmogenic spontaneous Ca^{2+} waves. At 22 °C, such waves are suppressed by intracellular acidosis, provided sarcolemmal acid-extrusion proteins are also inactive (Vaughan-Jones & Balnave, 2001). We have now examined the pH_i sensitivity of spontaneous waves at 37 °C.

Ventricular myocytes, isolated from rat (humanely killed by cervical dislocation), AM-loaded with Fluo-3, and Ca_i^{2+}-overloaded by raising $[Ca^{2+}]_o$ to 7.5 mM, were confocally imaged (Leica DM IRBE ×100 1.4 NA objective) in line-scan mode (100 μM line scanned at 450 Hz, excitation at 515 nm). pH_i was reduced by superfusion with 40 or 80 mM acetate. Data, collected during the second minute of acetate superfusion, were normalized to control measurements recorded over 1 min before acetate addition. All results are expressed as means ± S.E.M. *P* values given were calculated with Student's paired *t* test.

At 37 °C, reducing pH_i from 7.32 ± 0.02 ($n = 15$) to 6.82 ± 0.03 ($n = 8$) (measured in parallel experiments with intracellular carboxy SNARF-1) increased wave frequency by 341 ± 47 % ($n = 9$, $P < 0.05$). In comparison, at 22 °C a 0.74 pH unit decrease in pH_i increased spontaneous wave frequency ($P < 0.05$) by a smaller amount (210 ± 36 %; $n = 10$) (Vaughan-Jones & Balnave, 2001). At both temperatures in the presence of 30 μM cariporide (a selective cardiac Na^+–H^+ exchange (NHE-1) inhibitor) intracellular acidosis almost entirely suppressed wave formation.

At 37 °C decreasing pH_i from 7.32 to 6.72 (decrease of 0.6 pH units) enhanced average wave velocity from 75 $\mu m\ s^{-1}$ to 120 $\mu m\ s^{-1}$, i.e. by 150 ± 3 % ($n = 9$, $P < 0.05$). In the presence of 30 μM cariporide, there was still an increase in velocity (130 ± 15 %; $n = 3$). At 22 °C reducing pH_i by 0.74 pH units caused an even greater increase in velocity (176 ± 3 %; $n = 10$, $P < 0.05$), and this was again unaffected ($n = 7$) by inhibiting NHE-1.

In conclusion, during Ca_i^{2+} overload a fall of pH_i increases the frequency of spontaneous Ca^{2+} waves, an effect attenuated by moderate hypothermia. In the presence of cariporide, however, acidosis suppresses waves at both 22 °C and 37 °C. Intracellular acidosis increases the velocity of Ca^{2+} waves, an effect enhanced by hypothermia. This increase, however, is not influenced by cariporide and is therefore independent of NHE activity. The effect of intracellular pH on spontaneous Ca^{2+} waves thus depends on at least two mechanisms, one of which relies on the activity of sarcolemmal Na^+–H^+ exchange.

Balnave CD & Vaughan-Jones RD (2000). *J Physiol* **528**, 25–37.

Vaughan-Jones RD & Balnave CD (2001). *J Physiol* **533.P**, 25*P*.

This work was funded by the BHF and Wellcome Trust. We thank Dr H. W. Kleeman of Aventis, for kindly providing cariporide.

All procedures accord with current UK legislation.

PC28

Regulation of pH in equine chondrocytes

T.P.A. Fairfax*, R.J. Wilkins*, P. Milner†, M.E. Davies† and J.S. Gibson†

** Physiology, Parks Road, Oxford OX1 3PT and †Centre for Veterinary Science, Madingley Road, Cambridge CB3 0ES, UK*

Regulation of intracellular pH (pH_i), critical for all cells, is particularly important to articular chondrocytes, affecting turnover of cartilage matrix (Wilkins & Hall, 1995) and Ca^{2+} signalling pathways (Browning & Wilkins, 2002). Homeostasis of pH is therefore relevant to joint physiology. In addition, joint disease can result in perturbations of pH_i. Notwithstanding its importance, the mechanisms by which equine articular chondrocytes carry out pH regulation remain unknown. In this communication, we address the mechanisms by which equine chondrocytes respond to an acid load.

Cartilage slices were taken from equine metacarpophalangeal (fetlock) joints of horses killed humanely for other purposes and chondrocytes isolated following digestion with collagenase. pH_i was determined fluorimetrically at 37 °C using BCECF (see Wilkins & Hall, 1992). NH_4Cl was used to alter pH_i. Salines were buffered with Hepes (10 mM; HBS) or HCO_3^-/CO_2 (25 mM, 5 %; BBS). In some experiments, $[Ca^{2+}]_i$ was measured simultaneously using Fura-2 (Browning & Wilkins, 2002).

Under steady state conditions (pH_o 7.4) in HBS, pH_i was 7.18 ± 0.02 (mean ± S.E.M., $n = 6$). Following acidification (to approximately 6.70), pH recovered with a time constant of 26 ± 8 s ($n = 3$; Fig. 1, i). The recovery was inhibited by application of HOE694 (100 μM), a specific inhibitor of the Na^+/H^+ exchange isoform NHE-1. A small component (*ca* 19 %) was inhibited by NBD-Cl (100 μM), an inhibitor of H^+-ATPase. In BBS, pH recovery was greater (Fig. 1, ii), and a small but consistent rise in pH persisted in the presence of HOE694 (Fig. 1, iii). Intrinsic buffering capacity was *ca* 20 mmol (l cells)$^{-1}$ pH unit^{-1} at steady-state pH_i. Finally, when pH was increased (to *ca* 7.7), there was a parallel increase in $[Ca^{2+}]_i$ (*ca* 60 nM).

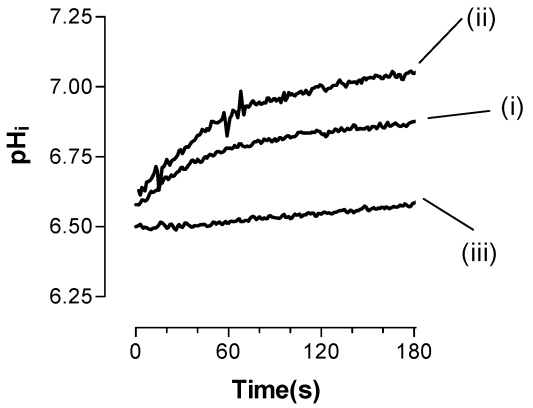

Figure 1. Intracellular pH in isolated equine chondrocytes (see text for details).

The results imply that, in equine chondrocytes, the major part of recovery from an acid load is mediated via NHE-1, with small contributions from H^+-ATPase and HCO_3^--dependent processes, i.e. HCO_3^-–Cl^- exchange and/or Na^+-dependent HCO_3^- transport. Finally, Ca^{2+} homeostasis is affected by pH_i. We hypothesise that a more complete understanding of pH homeostasis in equine chondrocytes may allow the development of future therapeutic regimes to protect against joint disease.

Browning JA & Wilkins RJ (2002). *Eur J Physiol* **444**, 744–751.

Wilkins RJ & Hall AC (1992). *Exp Physiol* **77**, 521–524.
Wilkins RJ & Hall AC (1995). *J Cell Physiol* **164**, 474–481.

We thank Pet Plan Charitable Trust, The Slater Fund (Cambridge University), the Sir Halley Stewart Trust and the Arthritis Research Campaign for financial support.

All procedures accord with current UK legislation.

PC29

The effect of post-natal development on tetrahydrocannabinol-induced activation of the apoptotic cascade in the rat cortex

Ingrid Redmond, Eric J. Downer and Veronica A. Campbell

Department of Physiology, Trinity College Institute of Neuroscience, Trinity College, Dublin, Ireland

Δ9-Tetrahydrocannabinol (THC), the psychoactive ingredient of marijuana, induces apoptosis in neurons prepared from neonatal rats (Downer *et al.* 2001) but not in adult neurons *in vivo* (Galve-Roperh *et al.* 2000). Our study aimed to examine the influence of post-natal development on the ability of THC to activate components of the apoptotic cascade (c-Jun N-terminal kinase (JNK), p53 and caspase-3) in the cortex.

Cortical slices (250 μm thickness) were prepared from humanely killed 1-day-old, 2-week-old and 3-month-old male Wistar rats and incubated with THC (5 μM) ± the CB_1 antagonist, AM-251 (10 μM), for 2 h at 37 °C in Hepes-buffered physiological saline. The activities of JNK and p53 were assessed by Western immunoblot using anti-phospho-JNK$^{Thr\text{-}183\ Tyr\text{-}185}$ and anti-phospho-p53^{Ser15} antibodies. Caspase-3 activity was assessed by analysis of the rate of cleavage of the fluorescent DEVD-AFC substrate peptide.

Age Group	p-JNK-1 Arbitrary units	p-JNK-2 Arbitrary units	p-p53 Arbitrary units	Caspase-3 (pmol AFC/mg/min)
1 day control	0.936 ± 0.151	0.484 ± 0.091	0.926 ± 0.213	4.21 ± 1.80
1 day THC	0.819 ± 0.124	0.657 ± 0.104	0.732 ± 0.179	43.04 ± 14.13*
2 week control	0.825 ± 0.346	1.286 ± 0.378	0.524 ± 0.064	2.11 ± 0.97
2 week THC	0.799 ± 0.124	1.310 ± 0.472	0.665 ± 0.163	1.11 ± 0.13
3 month control	0.679 ± 0.031	1.033 ± 0.123	2.043 ± 0.195*	0.40 ± 0.09
3 month THC	0.729 ± 0.094	1.43 ± 0.439	3.117 ± 0.646*	0.29 ± 0.02

Table 1. Influence of post-natal development on THC-induced activation of JNK, p53 and caspase-3. Results are expressed as means ± S.E.M. *$P < 0.01$, ANOVA, followed by Bonferroni test, $n = 6$.

In slices prepared from 1-day-old rats the stimulatory effect of THC on caspase-3 (Table 1) was abolished by AM-251 (caspase-3 activity was 4.05 ± 1.17 pmol AFC mg^{-1} min^{-1} in cells treated with THC + AM-251).

Thus, p-p53 expression was significantly increased in the cortex of 3-month old rats, although THC failed to modulate the activities of JNK1/2 or p53 in any of the age groups. However, the proclivity of THC to activate caspase-3, via the CB_1 receptor, was only observed in the neonatal cortex. This result suggests that the immature cortex may be more susceptible to the apoptotic effects of THC.

Downer *et al.* (2001). *Neuroreport* **12**, 3973–3978.
Galve-Roperh *et al.* (2000). *Nat Med* **6(3)**, 313–319.

This work was supported by the Health Research Board, Ireland.

All procedures accord with current National guidelines.

PC30

Neuroprotection by adenosine receptors in rat cortical neurons

N. Rebola, C.R. Oliveira and R.A. Cunha

Center for Neuroscience of Coimbra, Institute of Biochemistry, Faculty of Medicine, University of Coimbra, Portugal

Adenosine is a neuromodulator acting via four (A_1, A_{2A}, A_{2B} and A_3) receptors (Cunha, 2001). Adenosine is released in situations of metabolic stress and is considered a neuroprotective agent based on the ability of A_1 receptor activation to inhibit glutamate release, hyperpolarize neurons and decrease cellular metabolism (Cunha, 2001). Recent observations have highlighted the neuroprotective impact of A_{2A} receptor blockade in CNS stressful situations (Fredholm *et al.* 2003). However, it is unknown if the impact of the A_{2A} receptor on neuronal viability results from a direct action on neurons. Thus, we now used cultured neurons to test the effect of adenosine receptor agonists and antagonists on the outcome of neuronal viability.

Cerebral cortices were obtained from rat embryos (E15–16) and primary neurons were cultured for 6 days (Silva *et al.* 2001). They were then subjected to an excitotoxic stimulus (100 μM kainate plus 30 μM cyclothiazide) for 24 h, after which cell viability was assessed using syto-13 and propidium iodide (Silva *et al.* 2001). Adenosine receptor agonists and antagonists were added at least 30 min before the excitotoxic stimulus. All animals were humanely killed. The values are presented as means ± S.E.M. Statistical analysis was performed using Student's paired *t* test.

The excitotoxic stimulus led to a 42.7 ± 4.5 % ($n = 13$) neuronal death. Adenosine deaminase (2 U ml^{-1}, that converts adenosine into its inactive metabolite − inosine) reduced neuronal death to 33.5 ± 2.9 % ($n = 4$, $P < 0.05$, Student's *t* test). The A_1 receptor agonist, CPA (100 nM), had no effects on neuronal survival but the A_1 receptor antagonist, DPCPX (50 nM), decreased neuronal cell death to 30.7 ± 4.9 % ($n = 4$, $P < 0.05$). The A_{2A} receptor agonist, CGS 21680 (30 nM) reduced death to 25.8 ± 4.7 % ($n = 6$, $P < 0.05$) and this effect was prevented by the A_{2A} receptor antagonists, ZM 241385 (50 nM, $n = 4$) and SCH 58261 (50 nM, $n = 3$), which alone had no effect on neuronal viability. Finally, neither the A_3 receptor agonist, Cl^- IBMECA (100 nM, $n = 3$), nor the A_3 receptor antagonist, MRS 1191 (5 μM, $n = 3$), had any significant effect on neuronal survival.

These results indicate that in isolated neurons in culture adenosine has a neuroprotective effect, which is essentially due to removal of a noxious activation of A_1 receptors. Futhermore the activation rather than the blockade of A_{2A} receptors also protected neurons in accordance with what was shown in cerebral ischaemia in pups (Aden *et al.* 2003). This unexpected neuroprotective pattern of adenosine receptors in cultured cortical neurons might result from the different sensitivity to intracellular calcium of neurons from newborn rats (Turner *et al.* 2003), which indicates that neuronal cultures might not be adequate models to study neurotoxic phenomena in the adult brain.

Aden U *et al.* (2003). *Stroke* **34**, 739–744.
Cunha RA (2001). *Neurochem Int* **38**, 107–25.
Fredholm BB *et al.* (2003). *Curr Top Med Chem* **3**, 413–26.
Silva AP *et al.* (2001). *J Neurosci Res* **65**, 378–86.

Turner CP *et al.* (2003). *Exp Neurol* **178**, 21–32.

This work was supported by FCT.

All procedures accord with current National guidelines.

PC33

Differential expression of genes encoding voltage-gated K^+ channels in conduit *versus* resistance artery of mouse

S.J. Fountain, A. Cheong, A. Sivaprasadarao and D.J. Beech

School of Biomedical Sciences, University of Leeds, Leeds LS2 9JT, UK

Voltage-gated K^+ (Kv) channels play a critical role in the excitation–contraction coupling of arterial smooth muscle cells (Cheong *et al.* 2001*a,b*). A range of studies have indicated that the many genes encoding Kv channels may be differentially expressed in the vasculature, possibly because the different Kv channels serve different functional needs. However, quantitative data on expression are lacking. We used quantitative real-time RT-PCR to provide such data for murine aorta and first-order mesenteric artery.

Male 8-week-old C57/BL6 mice were killed humanely. Dissected arteries were endothelium-denuded by luminal perfusion with mild detergent. Aortic adventitia were removed by dissection. Kv RNA abundance was calculated as a ratio relative to β-actin RNA and taking into account primer-specific PCR efficiencies. Data are expressed as means ± S.E.M. and comparisons were made by Student's unpaired *t* test.

Levels of β-actin RNA (expressed as PCR crossing points, CP) were not significantly different between aortic medial layer, denuded aorta or denuded mesenteric artery (Cp 21.88 ± 0.32, 22.94 ± 0.20 and 22.18 ± 0.51; $P > 0.05$, $n = 4$–6). No significant differences were observed between aortae with or without adventitia or endothelium for all the Kv RNA species indicated below ($n = 4$, $P > 0.05$). Strikingly, Kv RNA levels were, however, orders of magnitude higher ($P < 0.05$ and $n = 4$ in each case) in mesenteric artery compared with aorta: Kv1.1 (1.46 ± 0.16 cf. 0.010 ± 0.002), Kv1.2 (0.06 ± 0.01 cf. 0.003 ± 0.001), Kv1.3 (0.05 ± 0.01 cf. 0.002 ± 0.000), Kv1.5 (0.03 ± 0.01 cf. 0.001 ± 0.001), and Kv2.1 (0.18 ± 0.03 cf. 0.044 ± 0.001). The RNA level for the Slo1 gene encoding the α-subunit of the large conductance calcium-activated K^+ channel was by contrast slightly, but not significantly ($P > 0.05$), less in mesenteric artery compared with aorta (0.43 ± 0.10 cf. 0.69 ± 0.11, $n = 4$ for each).

The data show that there is quantitatively much more expression of Kv channel genes in a resistance compared with a conduit artery. This is consistent with our hypothesis that Kv channel expression and function is important in resistance arteries and arterioles, and that relative and specific Kv channel gene expression patterns may have particular significance in the physiological control of blood pressure.

Cheong A *et al.* (2001*a*). *J Physiol* **534**, 691–700.

Cheong A *et al.* (2001*b*). *Am J Physiol* **281**, H1057–1065.

This work was supported by the Medical Research Council and the British Heart Foundation.

All procedures accord with current UK legislation.

PC33b

Vitamin C protects against the effect of high D-glucose on L-arginine transport and nitric oxide synthesis in human fetal endothelium

M. González*, P. Casanello*†, G. Vásquez*, J.D. Pearson‡, L. Sobrevia* and R.C.M. Siow‡

** Cellular and Molecular Physiology Laboratory (CMPL), Department of Obstetrics and Gynaecology & Medical Research Centre (CIM), School of Medicine, Pontificia Universidad Católica de Chile, PO Box 114-D, Santiago, Chile, † Department of Obstetrics and Gynaecology, Faculty of Medicine, University of Concepción, PO Box 160-C, Concepción, Chile and ‡ Centre for Cardiovascular Biology & Medicine, King's College London, London, UK*

Hyperglycaemia is associated with endothelial damage, a low cellular level of L-ascorbic acid, and increased L-arginine transport and eNOS expression and activity in human umbilical vein endothelial cells (HUVECs) (Beckman *et al.* 2001; Flores *et al.* 2003). Endothelial nitric oxide synthase (eNOS) activity is highly dependent on its redox state and is altered by reactive oxygen species (ROS) (Wang *et al.* 2001). L-Ascorbic acid has long been proposed as a major antioxidant and strong reducing agent, and a recent study suggests its role as an enhancer of NO bioactivity (Price *et al.* 2001). This study intended to determine the effect of L-ascorbic acid on L-arginine transport and eNOS protein expression and activity in HUVECs exposed to high D-glucose.

Cells isolated from normal pregnancies (Ethics Committee approval and informed patient consent were obtained) were cultured in medium 199 (containing 20 % bovine serum, 3.2 mM L-glutamine), and exposed (1 −24 h) to 5 or 25 mM D-glucose, in the absence or presence of L-ascorbic acid (0.1 −100 μM). L-Arginine transport (100 μM, L-[^{3}H]arginine, 2 μCi ml^{-1}, 37°C, 1 min) was determined in the absence or presence of L-ascorbic acid (100 μM). eNOS activity was determined by L-[^{3}H]citrulline formation from L-[^{3}H]arginine (4 μCi ml^{-1}, 30 min), and eNOS protein was detected by Western blot. mRNA for hCAT-1, hCAT-2B and eNOS was quantified by real-time PCR. ROS formation was characterized by measuring the fluorescence intensity of the ROS indicator 2′,7′-dichlorofluorescein (DCF).

High D-glucose increased the L-arginine transport (1.1 ± 0.02 *vs.* 0.4 ± 0.1 pmol (μg protein)$^{-1}$ min^{-1}, $n = 15$, $P < 0.05$, means ± S.E.M., Student's unpaired *t* test). L-Ascorbic acid blocked the effect of D-glucose on L-arginine transport (0.3 ± 0.1 pmol (μg protein)$^{-1}$ min^{-1}, $n = 4$, $P < 0.05$), with half-maximal effect at 0.3 ± 0.02 μM L-ascorbic acid, and at 3.5 ± 0.3 h incubation). In addition, D-glucose also increased ($P < 0.05$) L-citrulline synthesis (1.7-fold), eNOS protein (2.5-fold) and mRNA number of copies (2.4-fold), and hCAT-1 mRNA (2.3-fold) and hCAT-2B (2.6-fold) number of copies. The effects of D-glucose were blocked ($P < 0.05$) by L-ascorbic acid. Incubation of cells with 25 mM D-glucose increased ROS levels (1.5-fold) in HUVECs, but not in cells incubated with L-ascorbic acid.

In summary, D-glucose-induced alterations in the L-arginine–NO pathway in human umbilical vein endothelium could be due to higher levels of ROS, and L-ascorbic acid could act as a protective factor in hyperglycaemia.

This work was supported by FONDECYT (1030781, 1030607, 7030004, 7030109) and DIUC-University of Concepción (201.084.003-1.0)-Chile, and The Welcome Trust (UK).

Beckman JA *et al.* (2001). *Circulation* **103**, 1618–1623.

Flores C *et al.* (2003). *Circ Res* **92**, 64–72.

Price KD *et al.* (2001). *Atherosclerosis* **158**, 1–12.
Wang W *et al.* (2001). *Am J Physiol* **281**, C544–C554.

All procedures accord with current National guidelines and the Declaration of Helsinki.